

Effects of High Magnetic Fields on Cationic Exciton Lines in BiI_3

T. Komatsu and Y. Kaifu

Department of Physics, Faculty of Science, Osaka City University, Sumiyoshi-ku, Osaka 558, Japan

and

S. Takeyama and N. Miura

Institute for Solid State Physics, University of Tokyo, Roppongi, Minato-ku, Tokyo 106, Japan

(Received 10 July 1986)

A drastic energy shift and a growth of new splitting lines were observed in the magnetoabsorption spectra of stacking-fault excitons in BiI_3 under high pulsed magnetic fields up to 40 T. The observed magnetic field effects cannot be explained by a conventional effective-mass approximation or the bi-electron model, but were successfully understood on the basis of a model of cationic excitons which are perturbed by a specific stacking fault.

PACS numbers: 71.35.+z, 71.70.Ej, 78.20.Ls

Magneto-optical effects on excitons with a weak Coulombic binding, and thus a large radius of relative motion between electrons and holes, have been usually treated by the effective-mass approximation for a hydrogenlike envelope function (Wannier exciton case). A relatively low magnetic field is sufficient to investigate the internal structures of Wannier excitons in semiconductors.¹ However, there have been very few reports on magneto-optic effects on excitons with a strong (Frenkel exciton case) or an intermediate binding, which results in small radius. As the effects of the magnetic field are usually very small for such a system, a very high (megagauss) magnetic field is required to obtain an appreciable effect. However, if the exciton system has a narrow absorption linewidth with an appropriate optical density, even a small effect is detectable without using such extremely high fields.

Such an exciton system with an extremely narrow linewidth is observed below the indirect exciton edges in BiI_3 .² The lines of the group are named *Q*, *R*, *S*, and *T* from the high-energy side. In view of the fact that some of these lines fit well with inverse hydrogenlike series (IHS), Gross, Perel, and Shekhmametev³ have attributed these lines to the formation of a bielectron (or bihole). However, a strong sample dependence of the observed absorption lines suggested that they should be attributed to some defects in origin, and various difficulties in the bielectron model have been pointed out.⁴ Recently, the *R*, *S*, and *T* lines appearing near the indirect absorption edge have been clearly explained by excitonic transitions perturbed by a stacking fault formed between the layer planes.⁵ The lines are denoted as stacking-fault (SF) excitons.

In this paper, we present the first observation of internal energy structures for small-radius excitons under submegagauss fields by use of these specific SF excitons in BiI_3 . We discuss the obtained results on the basis of a model of band-edge cationic excitons perturbed by a

stacking fault. It will be shown that the sharp SF exciton lines are ideal systems to study the detailed internal structure of a bulk exciton state in applied magnetic field.

BiI_3 single crystals were grown by a sublimation method. As the magnetic field effects on the SF excitons are sample dependent, we carefully selected crystals having appropriate optical intensity and width of the absorption lines to obtain an optimum resolution in the magnetoabsorption (MA) spectrum. The MA spectra were measured at 4.2 K in pulsed high magnetic field up to 40 T.⁶ By use of an optical multichannel analyzer and optical fiber system, the whole absorption spectra were obtained at the flat part near the top of the pulsed magnetic field. The spectral resolution of this system was about 0.14 MeV.

Figure 1 shows MA spectra of the sharp absorption lines at 4.2 K. The MA spectra for the $[\mathbf{B}\perp\mathbf{z}, \mathbf{k}\parallel\mathbf{z}]$ configuration are shown for various field strengths. The inset of Fig. 1 shows a spectrum in the $[\mathbf{B}\parallel\mathbf{z}, \mathbf{k}\parallel\mathbf{z}]$ configuration as compared with the zero-field spectrum around the sharp absorption lines, where \mathbf{B} is the magnetic field, \mathbf{k} the wave vector of the incident light, and \mathbf{z} an axis in the direction of the layer stacking. In the $[\mathbf{B}\parallel\mathbf{z}, \mathbf{k}\parallel\mathbf{z}]$ configuration, the line shifts are very small (~ 0.2 meV at 31 T). However, it can be seen that the *R* line shifts to the higher-energy side and the *T* line shifts to the opposite side under high magnetic fields, while in the $[\mathbf{B}\perp\mathbf{z}, \mathbf{k}\parallel\mathbf{z}]$ configuration the *T* line shifts toward lower energy as the field is increased. The magnitude of the shift was -1.40 meV at 40 T. The MA spectra around the *S* line are found to be decomposed to a few peaks. The main line shifts slightly toward lower energies as the field is increased, and a new line appears on the higher-energy side of the main peak. The new line (called N_1) shifts toward a higher energy as the field is increased. The *R* line shifts slightly toward a lower energy and a new excitonic transition grows as the field

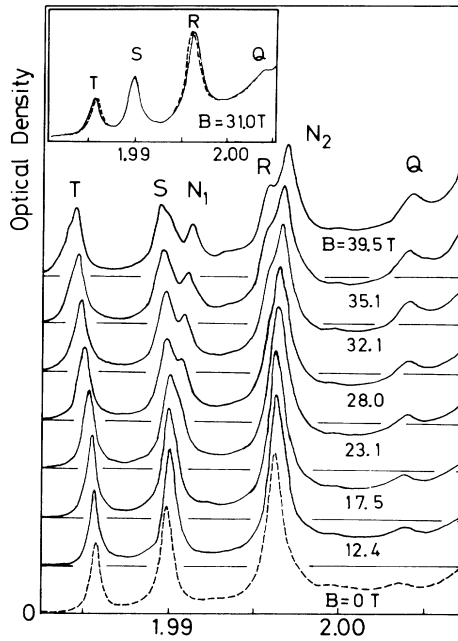


FIG. 1. Magnetoabsorption spectra for the sharp lines at 4.2 K. For the spectra of magnetic field dependence in the $[B \perp z, k \parallel z]$ configuration, growth of new lines can be seen on the higher-energy side of the S and R lines under high magnetic field. Note that the absorption intensity around R and Q lines increases with increasing magnetic field. Inset: The spectra in the $[B \parallel z, k \parallel z]$ configuration. Broken line is for data at zero field and solid line at 31 T. The energy shift for the R line is positive, while for the T line the shift is negative, and both shifts are comparable.

is increased. The new line (called N_2) shifts toward higher energies with increasing field.

These energy shifts for sharp lines are plotted as a function of the square of magnetic field in Fig. 2. It should be noticed that the magnetic field dependences of the SF-exciton lines are quadratic for the $[B \perp z, k \parallel z]$ configuration. The coefficient of the B^2 dependence is negative for the $R, S,$ and T excitons, while it is positive for the $Q, N_1,$ and N_2 lines. In Fig. 2, the energy positions for new lines N_1 and N_2 extrapolated to zero field do not coincide with those of the S and R lines at zero magnetic field. Thus, the new N_1 and N_2 lines are not attributed to the spin-split partners of the S and R lines. The oscillator strengths of the new lines also increase with magnetic field. As seen in the inset of Fig. 1, there is no obvious diamagnetic shift in the exciton spectra. Therefore, the present exciton system should have a very small radius as for the internal motion of electrons and holes. These results cannot be understood in a framework of degenerate Wannier-type $1s$ excitons in semiconductors.⁷

Figure 2 also shows experimental data reported by Starostin *et al.*⁸ for comparison. They observed similar

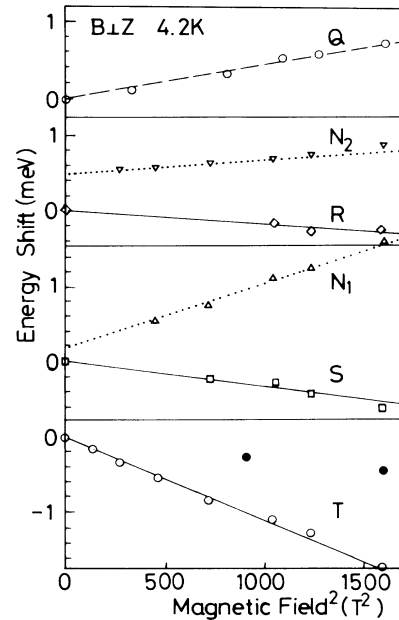


FIG. 2. Peak energy shifts as a function of square of magnetic field for T (open circles), S (open squares), R (lozenges), N_1 (triangles), N_2 (inverted triangles), and Q (circles). Two data points of the shift for the T line after Starostin *et al.* (Ref. 8) are shown by solid circles.

negative shifts with a quadratic field dependence for both the T line ($n=6$ in IHS) and the S line ($n=5$), and analyzed the results on the basis of a bielectronic diamagnetic shift, i.e., the negative shifts of both lines were ascribed to a negative reduced mass of bielectrons. However, the absolute values of the shift observed by Starostin *et al.* are very small compared with the present results. Moreover, we found that the shift of each line with magnetic field $B \perp z$ varies from sample to sample and also shows a dependence on the angle between the magnetic field and one of the crystalline axes in the layer plane. The discrepancy between the present result and that of Starostin *et al.*⁸ can be explained by the sample and angular dependences of the line shift. The shift of the R line is positive for $B \parallel z$ and negative for $B \perp z$, whereas the shifts of the T line are negative in both configurations. These sample-dependent anisotropic behavior of the SF exciton in magnetic fields cannot be interpreted in terms of bielectrons with a negative reduced mass.

In a previous paper, we proposed a model of stacking-fault responsibility for the sharp absorption lines.⁹ Such stacking faults in the BiI_3 lattice correspond to an interchange of positions of the cations and the anions through the fault plane, and causes two kinds of deformations on the relative positions of the cations in a unit cell containing the stacking-fault plane. One is weakly deformed and the other is strongly deformed. The former deformation occurs twice as often as the latter one. As the

exciton wave function is confined nearly in one unit cell, it is expected that the deformation alters the ground state of the bulk exciton and produces new exciton states at the stacking fault.

Similar splittings of the ground state of the exciton band have been observed in GaSe¹⁰ and PbI₂¹¹ crystals. The splitting in GaSe has been explained in a framework of the effective-mass approximation with a concept of localization of the large-radius exciton under finite coupling of the relative and center-of-mass motions. In BiI₃, the localization of the small-radius exciton should correspond to the transition just about the stacking-fault plane.

The valence and conduction bands of BiI₃ crystals have predominantly cation-admixture characters¹² similar to those of PbI₂ crystals.¹³ The bulk exciton transitions thus correspond to the excitation from *s* to *p* electronic states in the cation (Bi). The anisotropic exciton transitions observed in the reflection spectra have been interpreted by the cationic exciton model.¹⁴ The band-edge exciton states are composed of four states of triplet origin with an admixture of some singlet components caused by spin-orbit interactions. The prominent exciton transition at 2.07 eV (allowed in **E**⊥**z**) and the weak transition at 2.08 eV (**E**∥**z**) correspond to degenerate ψ_6 ($[x+iy]$ -like) and ψ_{10} ($[x-iy]$ -like) states and to ψ_3 (*z*-like) cationic exciton states, respectively. The ψ_4 state has an almost triplet character, and therefore is optically forbidden. These states are affected by the two kinds of deformations in a unit cell arising from a stacking-fault plane. This would result in two kinds of energy shifts and splittings of the degenerate states by mixing among the SF-exciton states as shown in Fig. 3. Theoretically, eight states are expected to be observed, but the actually observed states are six, the *Q*, *R*, *S*, *T*

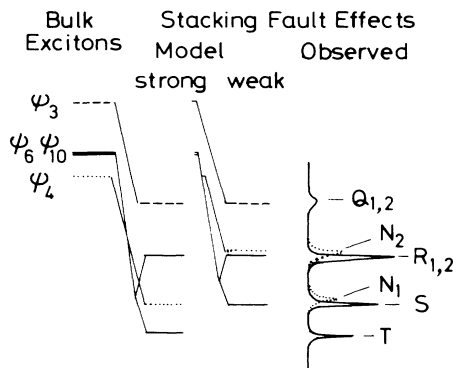


FIG. 3. Energy levels of the SF excitons originating from bulk exciton states consist of four states, ψ_3 , ψ_4 , ψ_6 , and ψ_{10} , which are shown on the left-hand side of the figure. Shifts and splittings of these four states by the two kind of deformations in a unit cell containing a stacking-fault plane are shown. As the weakly deformed cell occurs twice as often as the strongly deformed one, the levels corresponding to the former are indicated by double lines.

lines and N_1 , N_2 lines which grow up under magnetic fields. Therefore, some of the lines associated with the strongly and weakly deformed states must be degenerate. Since the *Q* line is weak and relatively broad compared with other lines, we can deduce that the *Q* line mainly consists of *z*-like and of nearly degenerate Q_1 and Q_2 which arise from two types of deformations. From the resonant Raman scattering studies on the sharp absorption lines, the *R* line can be regarded as another nearly degenerate line. A complete assignment thus obtained of the SF excitons is shown in Fig. 3. The Q_1 , R_1 , N_1 , and *T* lines correspond to ψ_{3SF}^s , ψ_{6SF}^s , ψ_{4SF}^s , and ψ_{10SF}^s states and the Q_2 , R_2 , N_2 , and *S* lines to ψ_{3SF}^w , ψ_{6SF}^w , ψ_{4SF}^w , and ψ_{10SF}^w states, respectively, where the indices *s* and *w* denote the states associated with the weak or strong stacking-fault effects.

The magnetic field effect can be calculated by a perturbation method, with the SF-exciton states as unperturbed states, and linear Zeeman terms as the perturbation. Nonzero off-diagonal matrix elements $\langle \psi_{jSF}^m | H_{\text{Zeeman}} | \psi_{kSF}^m \rangle$ cause a mixing among the SF-exciton states, where *m* refers to *s* or *w*. On the basis of the cationic exciton model, diagonal matrix elements of the orbital Zeeman term of the *p* electron remain nonzero in the **B**∥**z** configuration and off-diagonal elements contributed mainly by the spin Zeeman term remain in the **B**⊥**z** configuration. The sign is positive for ψ_6 and negative for ψ_{10} , which explains the experimental results in the **B**∥**z** configuration. In the **B**⊥**z** configuration, nonzero off-diagonal matrix elements give a quadratic dependence on magnetic field by a second-order perturbation. The sign of the shift is determined by the sign of the energy difference between mixing states in the energy denominator of the second-order term. A negative energy shift can be expected for the lower-lying states and a positive shift for the higher-lying states when the mixing occurs between two states. Thus, the N_1 and N_2 line shifts are positive, while the *T* and *S* line shifts are negative, and the absolute values of N_1 and N_2 line shifts are almost the same as those of the *T* and *S* lines, respectively. Thus, the results of a calculation on the basis of the cationic exciton model well explains the MA spectra of SF excitons in BiI₃.

The absorption band for bulk band-edge excitons has a very broad linewidth, which precludes an accurate measurement of the MA effects. In the present study, on the other hand, very sharp absorption lines of the SF excitons allowed precise measurements of the MA spectra. Though the experiments are performed for the SF excitons, the SF excitons originate from bulk excitons and thus their wave functions reflect those of bulk excitons. Therefore, from a good agreement between experiment and calculations based on the cationic model in the present study, we can deduce the cationic character of bulk band-edge excitons under a magnetic field. A model of cation-type exciton has been proposed by Habeke and Tosatti¹³ to explain the anomalous Wannier series of

excitons in $2H\text{-PbI}_2$ with use of the central-cell correction for the energy of the $1s$ exciton. The excitons in BiI_3 can be regarded as a characteristic prototype model of the cationic exciton. The present result of the MA spectra under strong magnetic field cannot be explained either by an exciton theory within effective-mass approximations or by a bielectron model with a negative reduced mass. Though the effective-mass approximation is invalid in this case, the mass of the exciton can be still considered on the basis of the recent discussion by Mattis and Galliner.¹⁵ A very large mass of indirect excitons along the layer-stacking direction in BiI_3 has been confirmed by resonant Raman scattering experiments.¹⁶ The large mass causes a strong localization of the excitons around a stacking fault, and this is a reason for the observation of surface-type excitons in BiI_3 ⁹ as in molecular crystals.¹⁷

The authors would like to express their sincere gratitude to Professor Yotaka Toyozawa for the continual encouragement throughout this work.

¹D. C. Reynolds and T. C. Collins, *Excitons: Their Properties and Uses* (Academic, New York, 1981), p. 31.

²Y. Kaifu and T. Komatsu, *J. Phys. Soc. Jpn.* **40**, 1377 (1976).

³E. F. Gross, V. I. Perel, and R. I. Shekhmametev, *JETP Lett.* **13**, 229, 357 (1971) [*Pis'ma Zh. Eksp. Teor. Fiz.* **13**, 320,

503 (1971)].

⁴Y. Kaifu, T. Komatsu, and T. Aikami, *Nuovo Cimento* **38**, 449 (1977).

⁵S. Tatsumi, T. Karasawa, T. Komatsu, and Y. Kaifu, *Solid State Commun.* **54**, 587 (1985); K. Watanabe, T. Karasawa, T. Komatsu, and Y. Kaifu, *J. Phys. Soc. Jpn.* **55**, 897 (1986).

⁶N. Miura, T. Goto, K. Nakao, S. Takeyama, T. Sakakibara, and F. Herlach, *J. Magn. Magn. Mater.* **54-57**, 1409 (1986).

⁷K. Cho, S. Suga, W. Dreybrodt, and F. Willmann, *Phys. Rev. B* **11**, 1512 (1975).

⁸N. V. Starostin, N. I. Ulitskii, B. M. Kharlamov, and R. I. Shekhmametev, *Sov. Phys. Solid State* **26**, 823 (1984) [*Fiz. Tverd. Tela (Leningrad)* **26**, 1354 (1984)].

⁹T. Komatsu, Y. Kaifu, T. Karasawa, and T. Iida, *Physica (Amsterdam)* **99B**, 318 (1980).

¹⁰J. J. Foney, K. Mashke, and E. Mooser, *J. Phys. C* **10**, 1887 (1977).

¹¹Le Chi Thanh, C. Depeuringe, F. Levy, and E. Mooser, *J. Phys. Chem. Solid* **36**, 699 (1975).

¹²M. Schlüter, M. L. Cohen, S. E. Kohn, and C. Y. Fong, *Phys. Status Solidi (b)* **78**, 737 (1976).

¹³G. Harbecke and E. Tosatti, *Phys. Rev. Lett.* **28**, 1567 (1972).

¹⁴T. Komatsu, Ph.D. thesis, Osaka City University, 1982 (unpublished).

¹⁵D. C. Mattis and J. P. Gallinar, *Phys. Rev. Lett.* **53**, 1391 (1984).

¹⁶T. Komatsu, T. Karasawa, K. Miyata, T. Iida, and Y. Kaifu, *J. Lumin.* **24/25**, 679 (1981).

¹⁷M. R. Philpott and J. M. Turllet, *J. Chem. Phys.* **64**, 3852 (1976).